IOSR Journal of Engineering (IOSRJEN)
e-ISSN: 2250-3021, **p**-ISSN: 2278-8719
Vol. 3, Issue 8 (August. 2013), ||V3 || PP 10-20

Degenerated Four Nodes Shell Element with Drilling Degree of Freedom

Fathelrahman. M. Adam[1], Abdelrahman. E. Mohamed[2], A. E. Hassaballa[3]
[1]*Dept. of Civil Engineering, Jazan University, Kingdom of Saudi Arabia*
[2]*Dept. of Civil Engineering, Sudan University of Science and Technology, Sudan.*
[3]*Dept. of Civil Engineering, Jazan University, Kingdom of Saudi Arabia*

Abstract: - A four node degenerated shell element with drilling degree of freedom is presented in this paper. The problem of zero stiffness that appears with using the drilling degree of freedom and causes singularity in the structure stiffness matrix is solved by employing, one of the recommended remedies. That is, adding a fictitious rotational stiffness using a penalty parameter (torsional constant) to control the solution to insure good element performance. Examples are presented including comparisons of torsional constant with the maximum displacements by using different mesh sizes, which results on selecting a value equal to one for the torsional constant is suitable value used to insure rapid convergence to true solution.

Keywords: - *Degenerated shell, drilling degree of freedom, fictitious rotational stiffness, Tensional constant.*

I. INTRODUCTION

Drilling or in-plane rotational, degrees of freedom have been introduced with various meanings and purposes to model displacements in planar finite elements. The need for membrane elements with drilling degrees of freedom arises in many practical engineering problems such as in-filled frames and folded plates. This special practice is frequently used in the analysis of thin shells by the finite element method. It is, basically, to allow correct modeling of the junction between angles of shell elements and to simplify the modeling of connections between plates, shells and beams, as well as the treatment of the junctions of the shells and box girders. Several work was initiated since 1964 for developing membrane finite elements with drilling degrees of freedom (Djermane (2006) [1] and Allman (1988) [2]). The assembly of the stiffness matrices of membrane and bending components at each node will result in a zero value on the diagonal corresponding to the drilling degree of freedom since this is not considered in the membrane or bending element as stated by Zeinkiewicz and Taylor (2000) [3], Alvin et al. (1992) [4], Felippa and Militello (1992) [5] and Felippa and Scot (1992) [6]. This zero stiffness for the drilling degree of freedom causes singularity in the structure stiffness matrix when all the elements are coplanar and there is no coupling between the membrane and bending stiffness of the element.

Several methods have been suggested by various authors for removing the singularity in the stiffness matrix based on variational principles such as those formulated by Gruttmann et al. (1992) [7]. These elements are stable and perform very well in non-linear problems. Knight (1997) [8] suggested that a very small value be specified for the stiffness of the drilling degrees of freedom so that the contribution to the strain energy equation from this term will be zero. Bathe and Ho (1981) [9] approximated the stiffness for drilling degrees of freedom by using a small approximate value. Batoz and Dhatt (1972) [10] presented the formulation of a triangular shell element named KLI element with 15 degrees of freedom and a quadrilateral shell element named KQT element with 20 degrees of freedom using the discrete Kirchoff formulation of plate bending element. The KQT element was developed by combining four triangular elements with the mid-nodes on the sides. The KQT element was found to be more effective among the two. Bathe and Ho (1981) [9] developed a flat shell triangular element by combining the constant strain triangle (CST) element for membrane stiffness and the plate bending element using the Mindlin theory of plates for the bending stiffness. They introduced a fictitious stiffness for the drilling degrees of freedom in the development of the element stiffness matrix for the triangular flat shell element. This element was found to be very effective for the analysis of shell structures. McNeal (1978) [11] developed the quadrilateral shell element QUAD4, by considering two in-plane displacements that represent membrane properties and one out-of-plane displacement and two rotations, which represent the bending properties. He included modifications in terms of a reduced order integration scheme for shear terms. He also included curvature and transverse shear flexibility to deal with the deficiency in the bending strain energy. The first successful triangles with drilling freedoms were presented by Allman in (1984) [12] and Bergan and Felippa in (1985) [13]. A degenerated shell element with drilling degrees of freedom was developed recently by Djermane *et al.* (2006) [1] for application in linear and nonlinear analysis of thin shell structures for isotropic or anisotropic materials with using the assumed natural strains technique to alleviate locking phenomenon. The

same authors extended the formulation by using the same techniques to study the dynamic responses of thick and thin nonlinear shells (Djermane *et al*. (2007) [14]).

Thus, the simplest method adopted to remove the rotational singularity is to add a fictitious rotational stiffness. However, Yang (2000) [15] suggested that, although the method solves the problem of singularity it creates a convergence problem that sometimes leads to poor results. A number of alternatives have been proposed by Adam and Mohamed (2013) [16] for avoiding the presence of this singular behavior. One of the remedies is to utilize the original penalty approach of Kanok–Kanukulchai (1979) [17], by introducing a constraint equation which "links" the drilling rotations in the fiber coordinate system to the in-plane twisting mode of the mid-surface. An additional energy functional can be then defined in the standard manner, to allow the application of the penalty method giving the preceding definition of the drilling degree of freedom with the fictitious torsional coefficient serving as a penalty parameter. Numerical experiments showed that the element performance is very sensitive to penalty parameter value as stated by Guttal and Fish (1999) [18].

In this paper a bilinear degenerated four nodes shell elements is developed. Five numerical examples are used to examine the element performance with respect to sensitivity to the value of penalty parameter and to evaluate the suitable value.

II. DEGENERATED FOUR NODES SHELL ELEMENT FORMULATION

This element was presented by Kanock-Nukulchai (1979) [17] under the following assumptions:
1. Normal to the mid-surface remains straight after deformation.
2. Stresses normal to the mid-surface are zero.

2.1 Geometric shape:

A four nodes element is obtained by degenerating the eight nodes solid element as shown in Fig. (2.1).

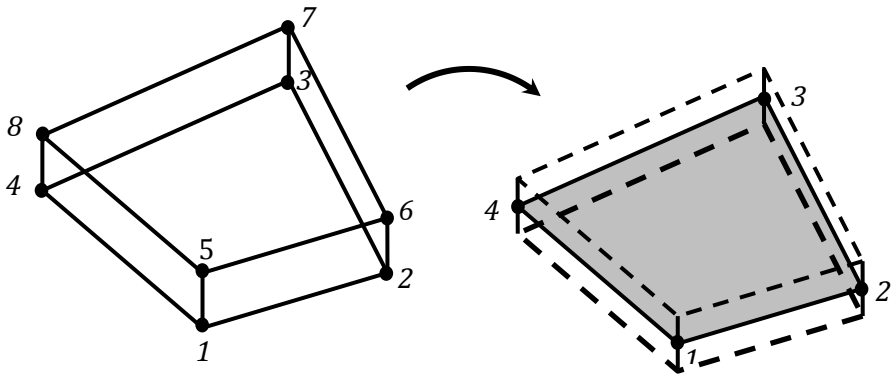

Fig. (2.1): Four nodes shell element degenerated from eight nodes solid element

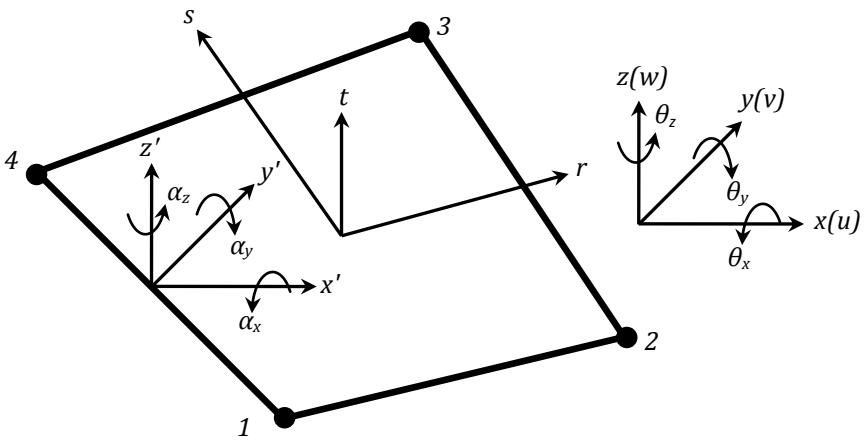

Fig. (2.2): Four nodes shell element

The midsurface shown in Fig. (2.2) is defined by natural coordinates (*r, s, t*). The displacements *u, v* and *w* are the displacements in global Cartesian coordinates *x, y* and *z* respectively. θ_x, θ_y, and θ_z are rotations about the *x, y* and *z* respectively. The rotations α_x, α_y and α_z are about local coordinates *x'*, *y*', and *z'* respectively.

The shape functions to describe the midsurface in terms of natural coordinates are:

$N_i\ (r,s) = ¼(1 + r_i\ r)\ (1 + s_i\ s)$ (2.1)

The thickness at each node h_i is computed in the direction normal to the midsurface.

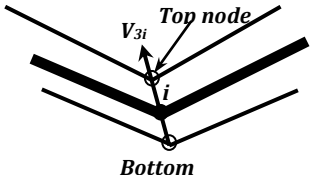

Fig.(2.3): Node director

From Fig.(2.3) vector $\boldsymbol{V_{3i}}$ is called node director and defined by:

$$\boldsymbol{V_{3i}} = \begin{Bmatrix} x_{itop} - x_{ibottom} \\ y_{itop} - y_{ibottom} \\ z_{itop} - z_{ibottom} \end{Bmatrix} \quad (2.2)$$

The coordinates of any point in the element can be derived from the 8-nodes solid element to 4-nodes element as:

$$\begin{Bmatrix} x \\ y \\ z \end{Bmatrix} = \sum_{i=1}^{4} \frac{1}{2}(1+t)\, N_i \begin{Bmatrix} x_i \\ y_i \\ z_i \end{Bmatrix}_{top} + \sum_{i=1}^{4} \frac{1}{2}(1-t)\, N_i \begin{Bmatrix} x_i \\ y_i \\ z_i \end{Bmatrix}_{bottom} \quad (2.3)$$

Since $\frac{1}{2}(1 \pm t)$ is the part of shape function in 8-nodes solid element in direction of the thickness.

and x_i, y_i and z_i are the global coordinates of the midpoint *i*

2.2 Displacement field:

The displacement variation in the element can be expressed as:

$$\begin{Bmatrix} u \\ v \\ w \end{Bmatrix} = \sum_{i=1}^{4} N_i \left(\begin{Bmatrix} u_i \\ v_i \\ w_i \end{Bmatrix} + \begin{Bmatrix} u_i^* \\ v_i^* \\ w_i^* \end{Bmatrix} \right) \quad (2.4)$$

Where u_i, v_i and w_i are the displacements at mid point *i* along global direction, and u_i^*, v_i^* *and* w_i^* are the relative nodal displacements along global direction produced by rotation of the normal at node *i* and can be expressed in terms of rotations θ_{xi}, θ_{yi}, and θ_{zi} at each node *i* about global axes. Using the assumption that straight normal to the midsurface remains straight after deformation, the displacements produced by the rotations α_{xi}, α_{yi} can be found as shown in Fig.(2.4) as:

$$\begin{Bmatrix} u_i' \\ v_i' \\ w_i' \end{Bmatrix} = \frac{t}{2} h_i \begin{Bmatrix} \alpha_{yi} \\ -\alpha_{xi} \\ 0 \end{Bmatrix} \quad (2.5)$$

where u_i', v_i' *and* w_i' are the displacements components along local axes at node *i*. To transform these displacements to global axes, transformation matrix $\boldsymbol{T}$ (Eqn.(2.6)) can be used.

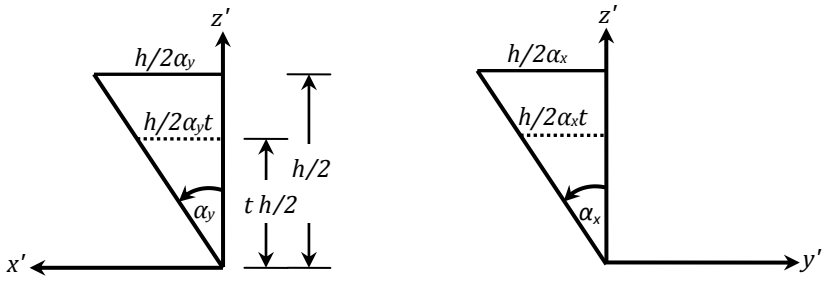

Fig. (2.4): Rotation of normal due to α_x and α_y

$$\boldsymbol{T} = \begin{bmatrix} l_1 & l_2 & l_3 \\ m_1 & m_2 & m_3 \\ n_1 & n_2 & n_3 \end{bmatrix} \tag{2.6}$$

where l_1, m_1 and n_1 (the direction cosines) are components of unit vector $\boldsymbol{v_1}$, and l_2, m_2 and n_2 are components of unit vector $\boldsymbol{v_2}$, and l_3, m_3 and n_3 are components of unit vector $\boldsymbol{v_3}$, then

$$\begin{Bmatrix} u_i^* \\ v_i^* \\ w_i^* \end{Bmatrix} = \boldsymbol{T_i} \begin{Bmatrix} u_i' \\ v_i' \\ 0 \end{Bmatrix}$$

$$= \frac{t}{2} h_i \begin{bmatrix} l_{1i} & -l_{2i} \\ m_{1i} & -m_{2i} \\ n_{1i} & -n_{2i} \end{bmatrix} \begin{Bmatrix} \alpha_{yi} \\ \alpha_{xi} \end{Bmatrix} \tag{2.7}$$

α_{xi} and α_{yi} are expressed in terms of global rotations θ_{xi}, θ_{yi}, and θ_{zi} by using transformation matrix $\boldsymbol{T_i}$ as:

$$\begin{Bmatrix} \alpha_{yi} \\ \alpha_{xi} \end{Bmatrix} = \begin{bmatrix} l_{2i} & m_{2i} & n_{2i} \\ l_{1i} & m_{1i} & n_{1i} \end{bmatrix} \begin{Bmatrix} \theta_{xi} \\ \theta_{yi} \\ \theta_{zi} \end{Bmatrix} \tag{2.8}$$

Substituting Eqn.(2.8) in Eqn.(2.7) gives:

$$\begin{Bmatrix} u_i^* \\ v_i^* \\ w_i^* \end{Bmatrix} = \frac{t}{2} h_i \begin{bmatrix} 0 & n_{3i} & -m_{3i} \\ -n_{3i} & 0 & l_{3i} \\ m_{3i} & -l_{3i} & 0 \end{bmatrix} \begin{Bmatrix} \theta_{xi} \\ \theta_{yi} \\ \theta_{zi} \end{Bmatrix} \tag{2.9}$$

And Substituting this in Eqn.(2.4), gives:

$$\begin{Bmatrix} u \\ v \\ w \end{Bmatrix} = \sum_{i=1}^{4} N_i \left(\begin{Bmatrix} u_i \\ v_i \\ w_i \end{Bmatrix} + \frac{t}{2} h_i \begin{Bmatrix} n_{3i}\,\theta_{yi} - m_{3i}\,\theta_{zi} \\ l_{3i}\,\theta_{zi} - n_{3i}\,\theta_{xi} \\ m_{3i}\,\theta_{xi} - l_{3i}\,\theta_{yi} \end{Bmatrix} \right) \tag{2.10}$$

2.3 Strain-displacement relation:

By assuming that the strain normal to midsurface $\varepsilon_{z'} = 0$, the strains components along the local axes are given by:

$$\begin{Bmatrix} \varepsilon_{x'} \\ \varepsilon_{y'} \\ \gamma_{x'y'} \\ \gamma_{x'z'} \\ \gamma_{y'z'} \end{Bmatrix} = \begin{Bmatrix} \dfrac{\partial u'}{\partial x'} \\ \dfrac{\partial v'}{\partial y'} \\ \dfrac{\partial u'}{\partial y'} + \dfrac{\partial v'}{\partial x'} \\ \dfrac{\partial u'}{\partial z'} + \dfrac{\partial w'}{\partial x'} \\ \dfrac{\partial v'}{\partial z'} + \dfrac{\partial w'}{\partial y'} \end{Bmatrix} \tag{2.11}$$

By splitting Eqn. (2.11) to two components, membrane component and shear component it can be rewritten as:

$$\begin{Bmatrix} \varepsilon_{x'} \\ \varepsilon_{y'} \\ \gamma_{x'y'} \end{Bmatrix} = (\boldsymbol{B_{m1}} + t\,\boldsymbol{B_{m2}})\,\boldsymbol{u} \tag{2.12}$$

$$\begin{Bmatrix} \gamma_{x'z'} \\ \gamma_{y'x'} \end{Bmatrix} = (\boldsymbol{B_{s1}} + t\,\boldsymbol{B_{s2}})\,\boldsymbol{u} \tag{2.13}$$

The matrices $\boldsymbol{B_{m1}}$, $\boldsymbol{B_{m2}}$, $\boldsymbol{B_{s1}}$ and $\boldsymbol{B_{s2}}$ can be derived by using Eqn. (2.14).

$$\frac{\partial u', v', w'}{\partial x', y', z'} = \boldsymbol{T_u} \frac{\partial u, v, w}{\partial x, y, z} \tag{2.14}$$

Where $\boldsymbol{T_u}$ is the transformation matrix needed to transform the derivatives of Eqn. (2.14).

2.4 Stress-strain relation:

The stress-strain relation can be stated after imposing $\sigma_{z'} = 0$ as:

$$\begin{Bmatrix} \sigma_{x'} \\ \sigma_{y'} \\ \tau_{x'y'} \\ \tau_{x'z'} \\ \tau_{y'z'} \end{Bmatrix} = \frac{E'}{1-\nu^2} \begin{bmatrix} 1 & \nu & 0 & 0 & 0 \\ \nu & 1 & 0 & 0 & 0 \\ 0 & 0 & \frac{(1-\nu)}{2} & 0 & 0 \\ 0 & 0 & 0 & \frac{\mu(1-\nu)}{2} & 0 \\ 0 & 0 & 0 & 0 & \frac{\mu(1-\nu)}{2} \end{bmatrix} \begin{Bmatrix} \varepsilon_{x'} \\ \varepsilon_{y'} \\ \gamma_{x'y'} \\ \gamma_{x'z'} \\ \gamma_{y'z'} \end{Bmatrix} \tag{2.15}$$

where $\mu = 5/6$ is a factor that accounts for the thickness-direction variation of transverse shear strain, E' is the modulus of elasticity and ν is Poisson's ratio.

The constitutive matrix in Eqn. (2.15) is split into $\boldsymbol{C_m}$ and $\boldsymbol{C_s}$ as follows:

$$\boldsymbol{C_m} = \frac{E'}{1-\nu^2} \begin{bmatrix} 1 & \nu & 0 \\ \nu & 1 & 0 \\ 0 & 0 & \frac{1-\nu}{2} \end{bmatrix}, \boldsymbol{C_s} = \frac{E'\mu}{2(1+\nu)} \begin{bmatrix} 1 & 0 \\ 0 & 1 \end{bmatrix} \tag{2.16}$$

2.5 Element stiffness matrix:

The stiffness matrix can be split into two matrices, membrane and bending effects and transverse shear effects and can be written as:

$$\boldsymbol{K_m} = \int_{-1}^{1}\int_{-1}^{1}\int_{-1}^{1} (\boldsymbol{B_{m1}} + t\,\boldsymbol{B_{m2}})^T\, \boldsymbol{C_m}\, (\boldsymbol{B_{m1}} + t\,\boldsymbol{B_{m2}})\, det\,\mathbf{J}\, dr\, ds\, dt \tag{2.17a}$$

$$\boldsymbol{K_s} = \int_{-1}^{1}\int_{-1}^{1}\int_{-1}^{1} (\boldsymbol{B_{s1}} + t\,\boldsymbol{B_{s2}})^T\, \boldsymbol{C_s}\, (\boldsymbol{B_{s1}} + t\,\boldsymbol{B_{s2}})\, det\,\mathbf{J}\, dr\, ds\, dt \tag{2.17b}$$

Integrating Eqn. (2.17)a and Eqn. (2.17)b directly across the thickness with respect to *t*, gives:

$$\boldsymbol{K_m} = \int_{-1}^{1}\int_{-1}^{1} \left(2(B_{m1}^T\, C_m\, B_{m1}) + \frac{2}{3}(B_{m2}^T\, C_m\, B_{m2}) \right) det\,\mathbf{J}\, dr\, ds \tag{2.18a}$$

$$\boldsymbol{K_s} = \int_{-1}^{1}\int_{-1}^{1} \left(2(B_{s1}^T\, C_s\, B_{s1}) + \frac{2}{3}(B_{s2}^T\, C_s\, B_{s2}) \right) det\,\mathbf{J}\, dr\, ds \tag{2.18b}$$

2.6 Torsional stiffness matrix

In a degenerated shell, the rotation of the normal and the mid-surface displacement field are independent. The idea then is to derive an additional constraint between the torsional rotation of the normal, α_z, and the rotation of the mid-surface, $\frac{1}{2}\left(\frac{\partial v'}{\partial x'} - \frac{\partial u'}{\partial y'}\right)$ [17].

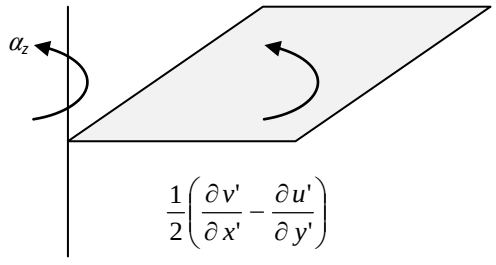

Fig. (2.5) Torsional rotation of the normal and midsurface

The derivation of the torsional rotation of the normal from that of the midsurface is assumed to have governing strain energy [4] and [17] as:

$$\boldsymbol{U_t} = \alpha_t G \int_A \int \left[\alpha_z - \frac{1}{2}\left(\frac{\partial v'}{\partial x'} - \frac{\partial u'}{\partial y'} \right) \right]^2_{(r,s,0)} dA$$

$$= \boldsymbol{u^T K_t u} \tag{2.19}$$

where α_t is the torsional constant and it is problem dependent, G is the shear modulus, and $\frac{\partial v'}{\partial x'}$ and $\frac{\partial u'}{\partial y'}$ can be calculated from Eqn. (2.14).

The matrix $\boldsymbol{B_3}$ can be written after extracting the vector of nodal displacements $\boldsymbol{u}$ from the relation $\left[\alpha_z - \frac{1}{2}\left(\frac{\partial v'}{\partial x'} - \frac{\partial u'}{\partial y'} \right) \right]$, then the torsional stiffness matrix is given by:

$$\boldsymbol{K_t} = \alpha_t G \int_{-1}^{1} \int_{-1}^{1} \left(B_3^T B_3 \right) dA \tag{2.20}$$

α_t is a penalty parameter and must be determined to insure good convergence.

III. NUMERICAL EXAMPLES

To examine the effects of torsional constant (α_t) in the solution, a program was developed for the degenerated shell element formulation and five numerical examples with different geometric shapes and different support conditions were employed using different values for α_t ranging from 1E-5 to 1E+5, with different mesh sizes and the resulting maximum displacements were recorded.

By plotting the displacements versus α_t using these meshes for the five Examples, the effect of α_t value, the rate of convergence and the suitable mesh size that gives a displacement value close to the exact value are determined.

Example 1: Pinch Cylinder Shell:

The thin circular cylindrical shell is subjected to equal and opposite point loads and the ends are restrained by rigid diaphragms as shown in Fig.(2.6) and for symmetry, only one octant of the cylindrical shell was modeled. the maximum displacements were plotted versus α_t using (4x4, 8x8, 12x12, 16x16, 20x20) mesh size as shown in Fig. (2.7).

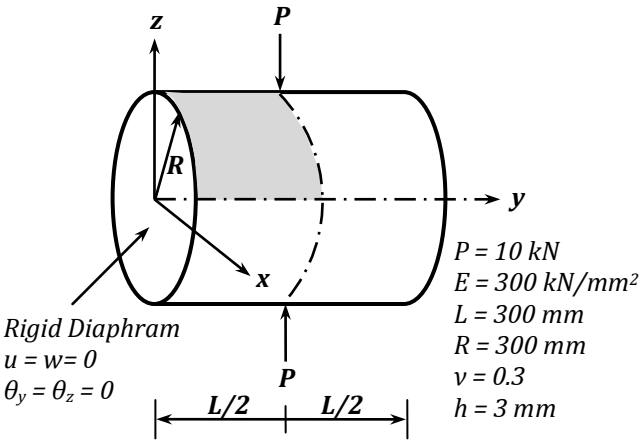

Fig. (2.6) Pinched Cylinder Shell

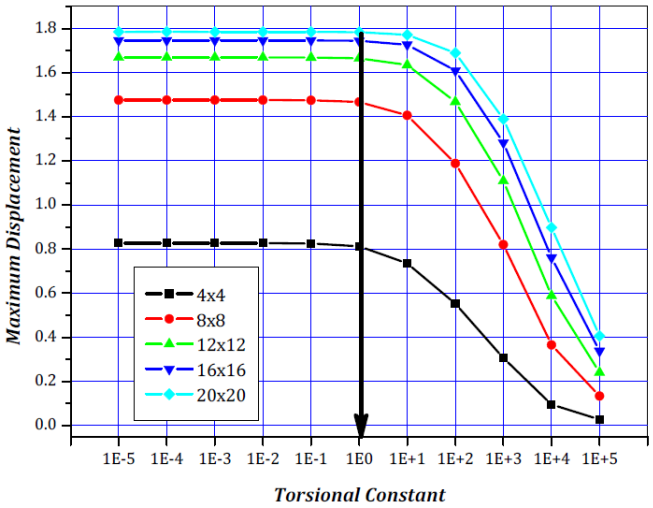

Fig. (2.7) Tensional Constant versus Maximum Displacement with Different Mesh Size for Example 1

Example 2: Scordelis-Lo roof:

The shell is supported on rigid diaphragms at the curved edge and free at straight edges and is loaded by its own weight and for symmetry, only one quarter of the roof shown in Fig. (2.8) was analyzed using (4x4, 8x8, 12x12, 16x16 and 20x20) meshes. The maximum displacements were plotted versus α_t for the different mesh sizes as shown in Fig. (2.9).

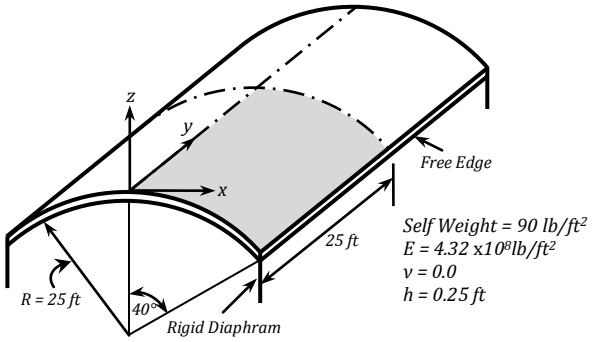

Fig. (2.8) Scordelis-Lo roof

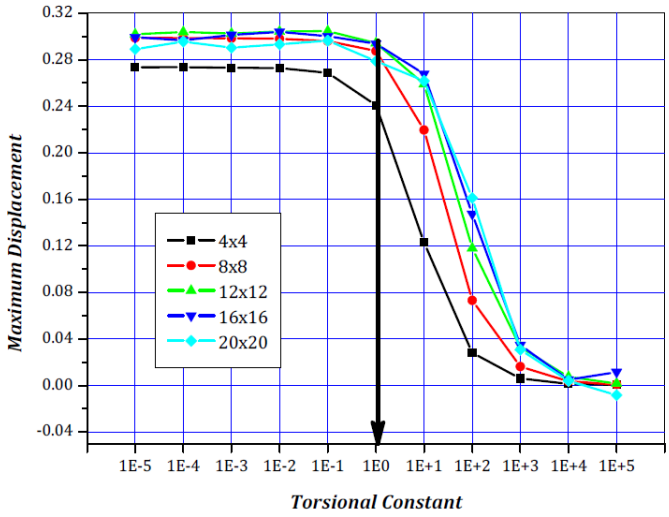

Fig. (2.9) Tensional Constant versus Maximum Displacement with Different Mesh Size for Example 2

Example 3: Short Cantilever Beam under End Shear Load:

A shear-loaded cantilever beam, as shown in Figure (2.10) was idealized using 4x2, 8x2, 16x4 and 32x8 element meshes. The maximum displacements were plotted versus α_t for the different mesh sizes as shown in Fig. (2.11).

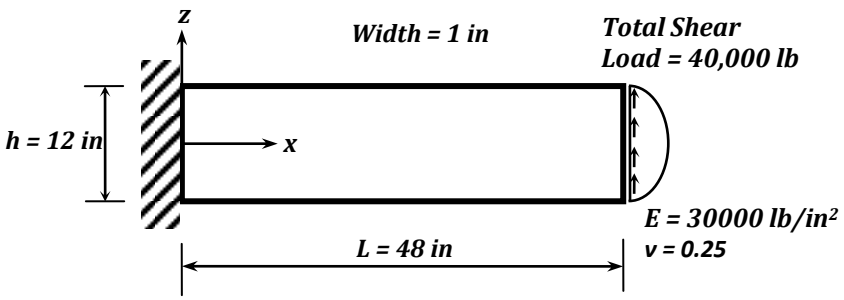

Fig. (2.10) Short Cantilever Beam

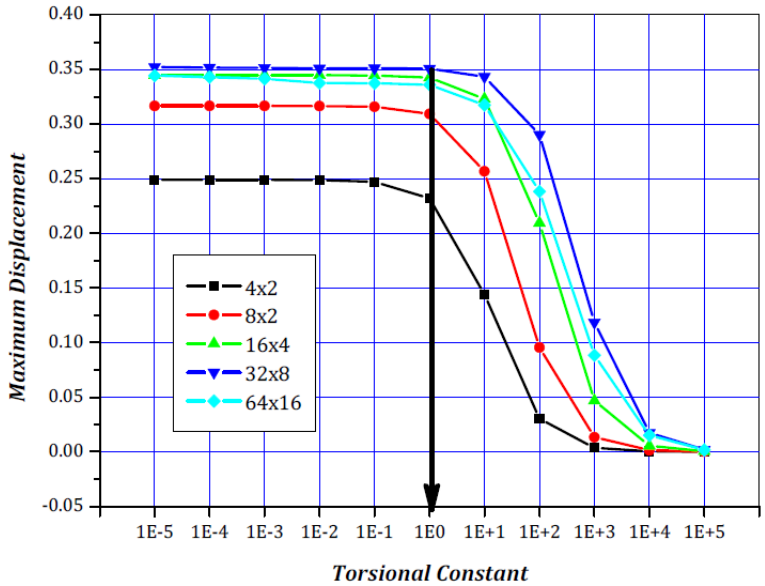

Fig. (2.11) Tensional Constant versus Maximum Displacement with Different Mesh Size for Example 3

Example 4: Folded plate simply supported on two opposite sides

The folded plate is simply supported on two opposite sides and is loaded by uniformly distributed load along the ridge. For symmetry, only one quarter of the shell was analyzed using (4x4, 8x8, 12x12, 16x16 and 20x20) meshes. The maximum displacements were plotted versus α_t for the different mesh sizes as shown in Fig. (2.13).

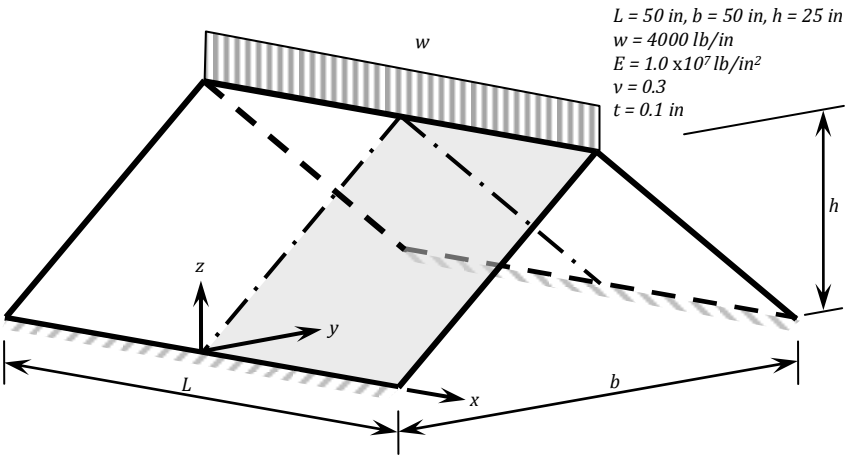

Fig. (2.12) Folded plate simply supported on two opposite sides

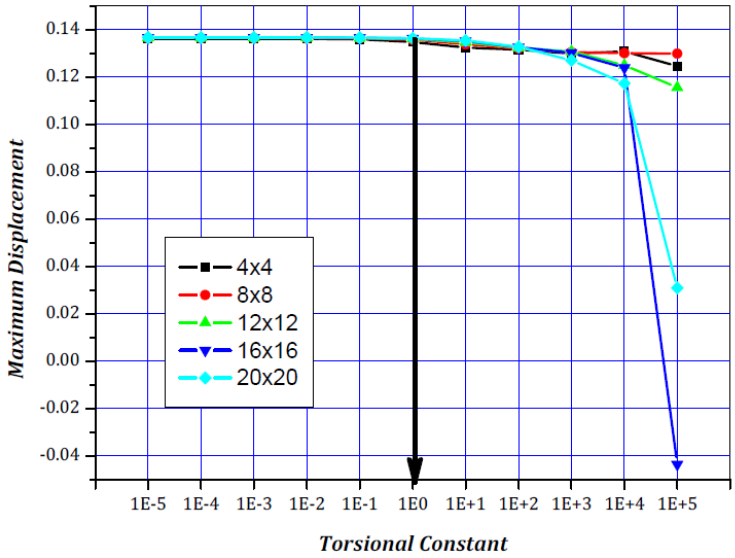

Fig. (2.13) Tensional Constant versus Maximum Displacement with Different Mesh Size for Example 4

Example 5: Clamped Hyperbolic Paraboloid Shell

The shell shown in Fig. (2.14) is the hyperbolic paraboloid shell and is clamped on four edges and subjected to a uniform normal pressure. For symmetry, only one quarter of the shell was modeled using (4x4, 8x8, 12x12, 16x16 and 20x20) meshes. The maximum displacements were plotted versus α_t for the different mesh sizes as shown in Fig. (2.15).

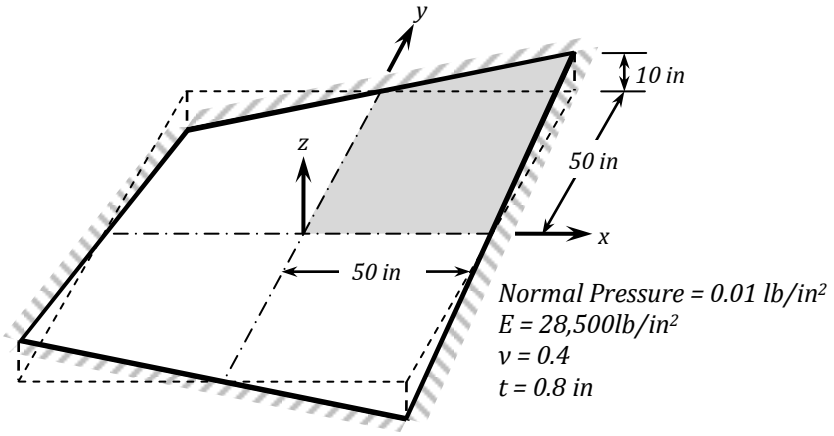

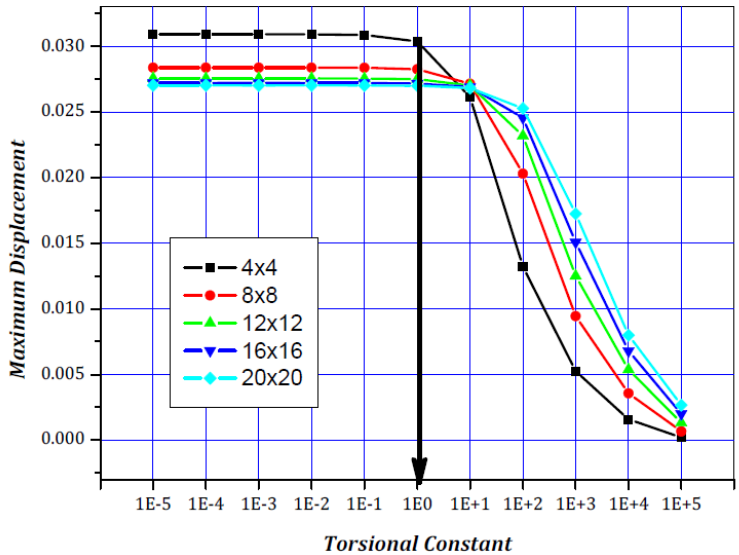

Fig. (2.15) Tensional Constant versus Maximum Displacement with Different Mesh Size for Example 5

IV. DISCUSSION

As can be seen from the plottings of the torsional constants versus maximum displacements using different mesh sizes for the five examples (figures 2.7, 2.9, 2.11, 2.13 and 2.15), using a small value, from 1 to 1E-5, for the torsional constant gives a high and constant value of maximum displacement which leads to rapid convergence. The displacement variation lines for the different meshes tend to be straight and parallel to the line of exact displacements starting from α_t equal to one. For values of α_t close to zero, while the displacements tend to close to the exact values, the values of rotations become very large instead of being close to zero which in turn affects the convergence of the solution. For larger values of torsional constant, greater than 1 and up to 1E+5, the value of maximum displacement decreases with increasing value of torsional constant which indicates poor convergence and results in wrong values of displacement. Thus, a value of 1 for the torsional constant is suitable for the degenerated four nodes shell finite element with six degrees of freedom and results in good convergence to the true solution.

V. CONCLUSION

This paper presents a formulation of the degenerated four nodes shell finite element with six degrees of freedom per node and drilling degree of freedom. A finite element program was developed and five examples were analyzed using the developed program. Solutions were obtained with different mesh sizes and variable torsional constant values in order to determine a suitable value for the torsional constant that can be used with torsional stiffness matrix. It can be concluded from the results obtained that:

1- The developed degenerated four nodes element with drilling degree of freedom resolves the stiffness singularity problem, provided the suitable value of torsional constant is used.
2- Values of torsional constants greater than one indicate poor convergence and lead to wrong results.
3- Small values, less than one, of the torsional constants, while resulting in displacement values close to the exact with rapid convergence, result in large rotation values instead of being close to zero, which in turn affects the convergence of the solution.
4- A torsional constant equal to one is the suitable value for good convergence to the true solution of results obtained using the four nodes degenerated shell element with drilling degree of freedom.

REFERENCES

[1]. Djermane, M., Chelghoum, A., Amieur, B. and Labbaci, B. (2006), *Linear and Nonlinear Thin Shell Analysis Using A Mixed Finite Element with Drilling Degrees of Freedom*, International Journal of Applied Engineering Research, Volume 1 Number 2 (2006) pp. 217-236

[2]. Allman, D.J. (1988), *A quadrilateral finite element iaeluding vertex rotations for plane elasticity analysis*, Internat. J. Numer. Meths. Engrg. 26 (1988) 717-730.

[3]. Zienkiewicz, O. C. and Taylor R.L. (2000), *The Finite Element Method*, Vol. 2, fifth edn., Butterworth-Heinemann, 2000.

[4]. Alvin K., de la Fuente H. M., Haugen B. and Felippa C. A. (1992), *Membrane Triangles with Corner Drilling Freedoms Part I: The EFF Element*, Finite Elements Anal. Des. 12, 163–187, 1992.

[5]. Felippa C. A. and Militello C. (1992), *Membrane Triangles with Corner Drilling Freedoms Part II: The ANDES Element*, Finite Elements Anal. Des. 12, 189–201, 1992.

[6]. Felippa C. A. and Scott A. (1992), *Membrane Triangles with Corner Drilling Freedoms Part III: Implementation and Performance Evaluation*, Finite Elements Anal. Des. 12, 203–235, 1992.

[7]. Gruttmann, F., Wagner, W. and Wriggers, P. (1992), *Nonlinear quadrilateral shells with drilling degrees of freedom*, Archive of Applied Mechanics 62, 1–13.

[8]. Knight Jr. N. F. (1997), *The Raasch Challenge for Shell Elements*, AIAAJ, Vol. 35, 1997, pp.375-388.

[9]. Bathe, K. J., and Ho, L. W. (1981), *A Simple and Effective Element for Analysis of General Shell Structures*, Computers and Structures, Vol. 13, pp. 673-681, 1981.

[10]. Batoz J. L. and Dhatt G. (1972), *Development of Two Simple Shell Elements*, AIAAJ, Vol. 10, No. 2, 1972, pp. 237-238.

[11]. McNeal R. H. (1978), *A Simple Quadrilateral Shell Element*, Computers and Structures, Vol. 8, 1978, pp. 175-183.

[12]. Providas E., Kattis M. A. (2000), *An assessment of two fundamental flat triangular shell elements with drilling rotations*, Computers and Structures 77, 129-139, 2000.

[13]. Felippa C. A. (2002), *A Study of Optimal Membrane Triangles with Drilling Freedoms*, Report CU-CAS-03-02, 2002.

[14]. Djermane M., Chelghoum A., Amieur B. and Labbaci B. (2007), *Nonlinear Dynamic Analysis of Thin Shells Using a Finite Element With Drilling Degrees of Freedom*, International Journal of Applied Engineering Research Vol. 2, No.1 pp. 97–108, 2007.

[15]. Yang H. T., Saigal S., Masud A., Kapania R. (2000), *A Survey of Recent Shell Finite Elements*, International Journal of Numerical Methods in Engineering, 2000, pp. 101-127.
[16]. Adam, F. M. and Mohamed, A. E. (2013), *Finite Element Analysis of Shell structures,* LAP LAMBERT Academic Publishing, *2013*
[17]. Kanok-Nukulchai, W. (1979), *A Simple and Efficient Finite Element for General Shell Analysis*, Int. J. Num. Meth. Engng, 14 ,pp. 179-200
[18]. Guttal, R. and Fish, J. (1999), *Hierarchical assumed strain-vorticity shell element with drilling degrees of freedom*, Finite Elements in Analysis and Design 33 (1999) 61-70
[19]. Jensen, L. R., Rauhe, J. C. and Stegmann, J. (2002), *Finite Element for Geometric Nonlinear Analysis of Composite Laminates and Sandwich Structures*, Master's Thesis, Institute of Mechanical Engineering Aalborg University, 2002.
[20]. Kansara, K. (2004), *Development of Membrane, Plate and Flat Shell Elements in Java*, M.sc. Thesis, Faculty of the Virginia Polytechnic Institute & State University, 2004.